EXPERIMENTS ON WATER HAMMER INDUCED BY FAST OPENING VALVE DURING PRIMING: EFFECT OF GAS DESORPTION

Marcos Lema[*1], **Fernando López Peña**[1], **Jean-Marie Buchlin**[2], **and Johan Steelant**[3]

[1] *University of A Coruña, 15000 A Coruña, Spain*
[2] *von Karman Institute for Fluid Dynamics, 1640 Rhode-St-Gense, Belgium*
[3] *ESA-ESTEC, 2200 AG Noordwijk, The Netherlands*

KEYWORDS: priming; fluid hammer; water hammer; two-phase flow; cavitation; gas desorption; flow visualization

ABSTRACT

This paper presents an experimental facility modeling a spacecraft propulsion system, where the physical phenomena taking place during priming are reproduced. This is achieved by discharging a test liquid into a propellant line kept under vacuum conditions. This configuration induces a high acceleration of the flow before going to rest at the closed end, inducing the subsequent water hammer pressure raise. Furthermore, the saturation level of the test liquid with the pressurant gas can be controlled, in order to characterize the influence of gas desorption during priming. Together with the unsteady pressure measurements, the facility mounts a transparent module, where the last segment of the propellant line is replaced by a quartz cylinder drilled with the same tube diameter. In this way, the flow can be recorded with high speed imaging at the impact location allowing characterizing the multiphase nature of the flow.

1. INTRODUCTION

When a satellite is launched to space, for security reasons its propulsion system is initially inactive. At this stage, the propellant lines are vacuum pumped and the liquid propellant is confined in the tanks, and isolated from the nozzles and catalyst beds by three valves, as sketched in figure 1. Once the spacecraft has been ejected from the launch vehicle, the first isolation valve opens and the evacuated propellant lines are filled with pressurized liquid propellant. This maneuver is called “priming” and is carried out by the fast opening of a pyrotechnic valve. The presence of a closed end in a piping system generally generates a water hammer when the flow is brought to rest. This scenario is particularly hazardous when a liquid flows into an evacuated pipe segment, that induces a high acceleration of the flow before going to rest, ant the subsequent water hammer pressure raise. Due to this physical configuration, the water hammer taking place involves several multiphase phenomena. In particular, the propellant is pressurized in the tank with a non-condensable gas (NCG) that dissolves in the liquid during storage. When the valve opens, the new pressure conditions are below the saturation pressure, inducing the desorption of the NCG, and if the pressure in the line are also below the vapor pressure, the liquid undergoes cavitation.

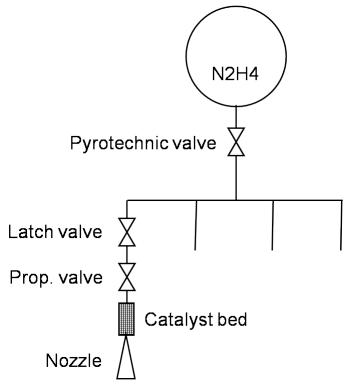

Figure 1. Monopropellant propulsion system configuration

Due to the complexity of these multiphase phenomena occurring in spacecraft hardware, there are very few literature references describing experiments with all the specifications of the above configuration, which are necessary for a proper validation of the physical models implemented in the CFD codes. Nowadays, various numerical codes are able to accurately predict the liquid compressibility effects when computing a single-phase fluid hammer but they still need to be extended and calibrated

[*] marcos.lema@udc.gal

for cases with cavitation and two-phase flows. Furthermore, the numerical treatment of a dissolved NCG in the liquid phase needs to be improved. In both cases, the existence of a well documented experimental database is mandatory for the improvement and validation of these physical models. Even though it is possible to find numerous studies dedicated to the fluid hammer, the references dealing with the priming process are not so numerous and the data available is not sufficient for validation purposes.

The studies available in the literature dealing with the priming process use both experimental and theoretical/numerical approaches, applied to simplified test configurations or to the whole propulsion system. In most of the cases, the authors tried to evaluate the adiabatic compression of the liquid, which may cause the explosive decompositon of the propellant, or the integrity of the piping system facing water hammer pressure surges. We can highlight the studies from Yaggy [1], Prickett et al.[2], Molinsky[3], Martin et al.[4], Joh et al.[5] and Morgan[6]. The main conclusions given by these studies are: unsteady friction plays an important role, the two-phase phenomena are directly linked to the pressure surge amplitude and water can replace MMH (monomethylhydrazine) as test fluid, producing pressure surges slightly higher than MMH, therefore making the studies conservative. Several authors attempted to model the priming process using dedicated numerical tools, such as Lin and Baker[7], Navickas et al.[8], Ounougha and Colozzi[9], Leca et al.[10] and Hern[11]. In most cases, the simulations have been carried out doing 1D computation where two-phase phenomena were not taken into account.

Two references are closely related to the present study, Gibek and Maisonnneuve[12] and Lecourt and Steelant[13], where the main objectives were to model experimentally the priming process taking place in satellites and to create an experimental database for validation purposes. In both studies both inert fluids and real propellants (MMH and nitrogen tetroxide) were used. The authors concluded the existence of a boiling front from the start, resulting in a local two-phase mixture of vapour and liquid. Furthermore, the NCG initially present in the test pipe gets compressed when the valve opens and the liquid front travels downstream. Since this compression occurs very fast, it is mainly adiabatic at the boundaries, producing an intense mixing and heat transfer at the multiphase liquid-vapour/NCG front. Lecourt and Steelant[13] also studied in detail the evolution for the first pressure peak, where a multiple step evolution before reaching the maximum pressure value was observed, and provided some hypothesis to explain this behaviour.

2. EXPERIMENTAL FACILITY

A new experimental facility has been built at the von Karman Institute (Belgium) and includes all the elements of a satellite propulsion system directly involved in the fluid hammer occurrence: a pressurized liquid tank, a fast opening valve (FOV) and a given length of pipe line. The main objective during the design phase was to conceive a facility without singular elements such as elbows and T-junctions upstream of the FOV, and with the same inner diameter in every component. It is well known that these geometrical singularities create secondary pressure waves, which complicate the interpretation of the general pressure measurements. Furthermore, the absence of these elements considerably simplify numerical modeling and result validation when applying CFD codes.

The facility layout is shown in figure 2, which is intended to be clamped to a vertical wall. The main components are a test vessel of $4\,l$, a fast opening valve (FOV), and a given length of the propellant line, referred to as “test element”. The fast opening valve used in this study consists of a ball valve with an orifice of $6\,mm$, equipped with a pneumatic actuator that allows to open the valve in the range of $45 - 50\,ms$. The line is made with the same titanium tube (alloy T3AL2.5V, specification AMS4943H) with $0.25\,in$ $(6.35\,mm)$ of inner diameter and $0.016\,in$ $(0.4\,mm)$ thickness, and following the same construction rules used for aerospace applications. Three test element configurations are proposed: straight, 90° elbow and T-bifurcation, but only results with the straight line are considered in this paper. The facility also includes a vacuum system to set the test conditions: test element initially vacuum pumped or filled with a NCG gas at different pressure levels. The vacuum system is connected to the line, upstream the FOV, with a T-junction and, like in any vacuum system, a buffer tank is installed at the pump inlet to avoid any liquid flow from being aspirated by the pump. A more detailed description of the facility and the test procedure can be found elsewhere by the same authors [14].

The test vessel is a spherical accumulator that mounts an elastic membrane. The purpose of the membrane is to avoid the absorption of the NCG during the liquid pressurization, allowing to run experiments with deaerated liquid or, when the driving pressure gas is mixed with the liquid, with fully saturated liquid. These test results provide very useful information to understand how the dissolved gas affects the fluid hammer mechanism. Furthermore, since the working liquid is saturated with air at standard conditions during storage, the fluid needs to be deaerated to run experiments without any dissolved gas. This is achieved by means of a depressurization process using a second $10\,l$ spherical accumulator, called deareation vessel, connected to

the vacuum pump. The dissolved gas is removed by keeping the liquid in a low-pressure atmosphere. This facility allows working with inert fluids and nitrogen as driving pressure gas.

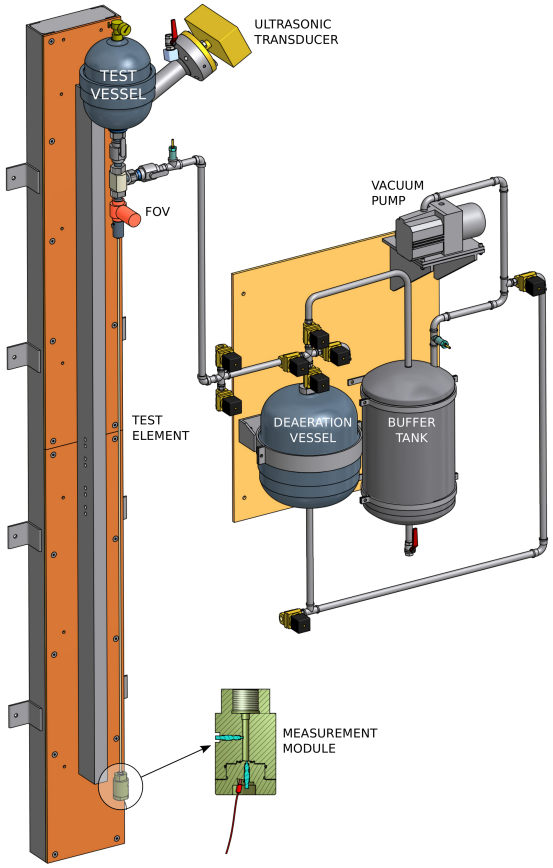

Figure 2. Experimental facility layout

The characterization of the pressure front induced by the fluid hammer is achieved through interchangeable measurement modules attached to the bottom end of the test element. Results with the instrumented module mounting unsteady pressure transducers can be found elsewhere by the same authors [14].

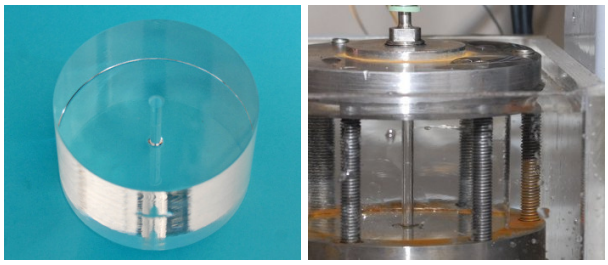

Figure 3. Transparent module

The results presented in this paper were obtained with the second module used in this study (figure 3), which is made out of quartz for flow visualization with high speed imaging. The module consists of a $50\,mm$ length cylinder, with a diameter of $100\,mm$, and with a drilled hole on the axis having the same internal diameter as the titanium tube. This solution was adopted due to the difficulties in drilling and polishing a $1/4''$ hole. The mounting of the module is achieved by two steel discs, enclosing the cylinder with six bolts. The top disc is also drilled with a thread that is screwed to the test element end, as figure 3 shows. In order to avoid the light distortion produced by the cylinder curved surface, the whole module is immersed in a water container, whose walls are made out of Plexiglas. In this way, the light distortion is avoided because the camera focuses on a flat wall of the container, whereas quartz, water and Plexiglas have nearly the same light refraction index.

3. WORKING FLUIDS AND TEST CONDITIONS

Results obtained with three inert fluids are presented: water, ethanol and acetaldehyde, and using the $2\,m$ straight configuration of the test element. These liquids are used instead of real propellants, such as monomethylhydrazine (MMH) and Nitrogen tetroxide (NTO), both commonly used as hypergolic propellant combination in rocket engines. These propellants are corrosive, toxic and carcinogenic, and their manipulation involves expensive safety precautions. For these reasons, they have never been considered as test fluids in the present study.

Table 1 summarizes the physical properties involved in water hammer occurrence (density, ρ, and wave velocity, c), multiphase behavior of the flow (liquid saturation pressure, P_v, and surface tension, σ), and friction (viscosity, μ). Water has similar values of density, viscosity and wave velocity to MMH, but with half the vapor pressure and a surface tension value twice as large. Ethanol has a similar vapor pressure and viscosity values to those of MMH, and similar speed of sound and surface tension to NTO. Acetaldehyde has the closest viscosity to that of NTO, with similar vapor pressure, speed of sound and surface tension. It is worth mentioning that NTO density is higher than in any test liquid used in this study.

The three liquids are pressurized at $2\,MPa$ in the test vessel, using nitrogen as driving pressure gas. Thanks to the deaeration process and the membrane inside the test vessel, the test liquid can be either fully saturated with the driving pressure gas or deaerated. Prior to the filling of the test vessel, the air dissolved in the liquid at standard conditions ($1\,atm$ and $293\,K$) is removed. This is achieved by half filling the deaeration vessel with the test liquid and applying a low pressure to the internal volume.

	MMH	Water	Ethanol	Acetaldehyde	NTO
$\rho\,[kg/m^3]$	875	998	789	783	1447
$\mu\,[Pa\cdot s]$	0.000855	0.001	0.00144	0.00023	0.0004
$c\,[m/s]$	1568	1487	1176	1141	1004
$P_v\,[Pa]$	4908	2300	5950	101300	90710
$\sigma\,[mN/m]$	33.83^*	72.85	22.27	21.2	27.5
$h_{lv}\,[kJ/kg]$	190	2453.8	1030	584	415
$C_{p,l}\,[kJ/kg\ K]$	2.850	4.182	2.40	2.02	1.565
$C_{p,g}\,[kJ/kg\ K]$	-	1.874	1.40	1.26	-

Table 1. Physical properties of inert test fluids and propellants in liquid phase at $293\,K$ *(*value at* $298.15\,K$*)*

In order to avoid the boiling of the test liquids at ambient temperature, the pressure applied is kept above their vapor pressure.

When we want to run experiments with deaerated liquid, before injecting the liquid into the test vessel, the line between the deaeration vessel and the test vessel is vacuum pumped, moving down the membrane and leaving a negligible amount of gas in the line. In case we want to saturate the liquid with the driving pressure gas, nitrogen is blown in the line and in the test vessel. In this way, the membrane moves upwards and fills the tank with gas. When the liquid is injected into the test vessel, it will be in contact with a bubble of nitrogen, allowing the saturation of the liquid with this gas during pressurization.

4. FLOW VISUALIZATION

Due to the flow configuration in satellite propellant lines, it is assumed that a two-phase flow evolves during priming. This can be concluded from the pressure evolution in the pipe. Nevertheless, a direct observation of the phenomenon is still missing. This is not evident due to the high pressure transients we are dealing with and a short characteristic time in the order of milliseconds. The solution proposed in this study allows the visualization of the flow at the bottom end, where the liquid front is brought to rest and the fluid hammer is induced. The image recording is achieved by means of a high speed camera. The image window resolution is set to 64×456 pixels, which allows capturing images at a maximum frame rate of 7005 pps.

The results of flow visualization will be now presented based on the most representative snapshots recorded at the impact location. The snapshots presented hereafter are extracted from the time lapse between the FOV opening and the second pressure peak, which show the most interesting features taking place during fluid hammer occurrence. The images are presented chronologically from left to right and top to bottom, and they are accompanied by the pressure evolution obtained with the instrumented measurement module to help on the understanding of the whole fluid hammer process.

4.1. Results with deaerated liquids

In figure 4, the results obtained with deaerated water are presented when the vacuum level in the pipe line is $P_p = 1\,kPa$. In the first snapshot, the FOV is still closed and the test element is vacuum pumped. A few instants after the valve starts to open, dispersed droplets arrive to the bottom, followed by visible liquid pockets in snapshot 2. The foamy mixture of liquid, vapor and NCG preceding the liquid front arrival appears dark colored in the images, as it can be clearly observed in snapshot 3. Here, the gas in the mixture comes from the residual NCG initially left in the line. Finally, the liquid front arrives and the induced pressure rise starts to condense the vapor phase and compresses the NCG dissolved in the liquid, as can be observed in snapshot 4.

When the pressure reaches its maximum, and for the duration of the pressure peak, the module appears full of liquid, as in snapshot 5. In this case, the images appear completely white. When the reflected expansion wave from the tank approaches the bottom end, the pressure decreases almost instantaneously at this location and the NCG starts to expand, inducing a bubbly flow. This can be observed in snapshot 6, where tiny gas bubbles grow within the liquid. The pressure drop is accompanied by the liquid column acceleration towards the tank, inducing the liquid column separation at the bottom end. The column separation leaves behind a foamy mixture of liquid, vapor and NCG (referred to as multiphase bubble), identified in snapshot 7. As the col-

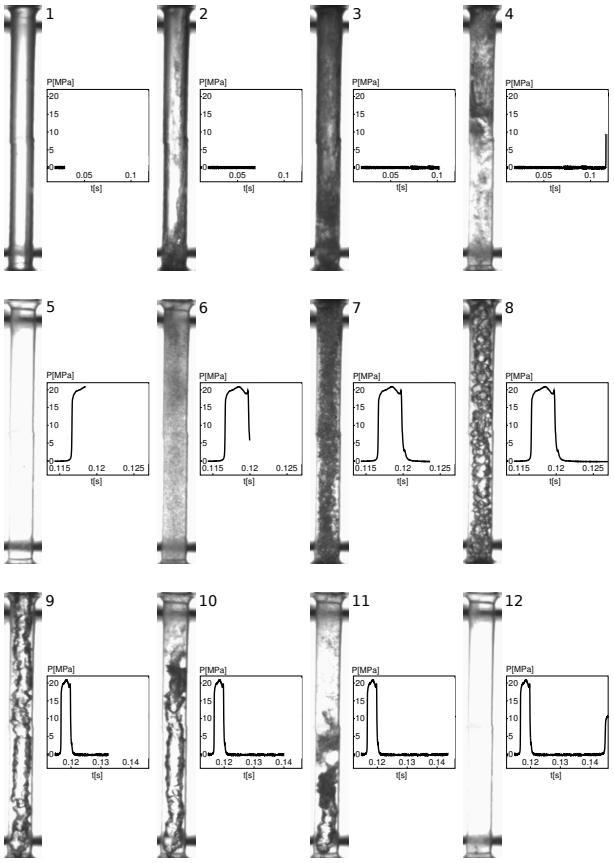

Figure 4. Liquid front visualization obtained with deaerated water in the straight configuration. Test conditions: $P_T = 2\,MPa$ *and* $P_p = 1\,kPa$

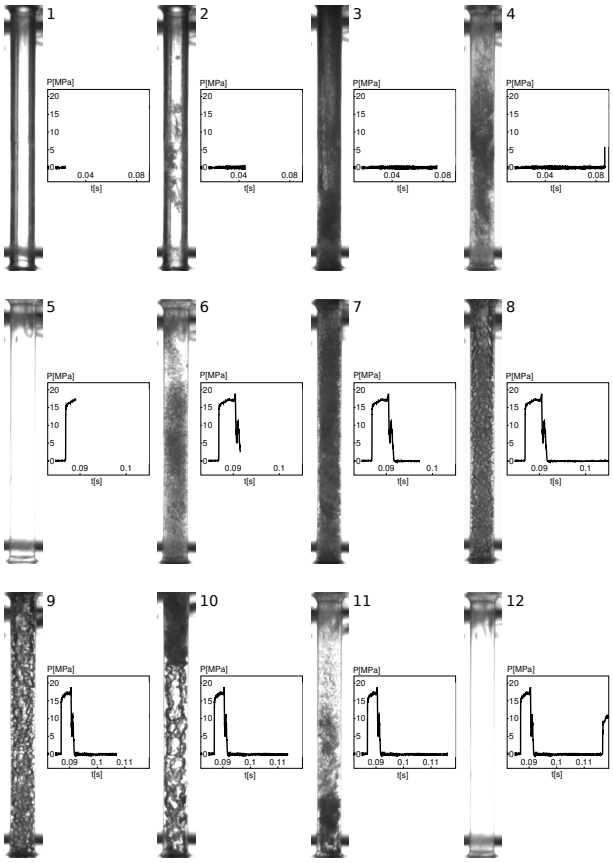

Figure 5. Liquid front visualization obtained with deaerated ethanol in the straight configuration. Test conditions: $P_T = 2\,MPa$ *and* $P_p = 1\,kPa$

umn continues moving towards the tank, the volume occupied by the multiphase mixture grows, inducing the coalescence of the gaseous bubbles, as can be already distinguished in snapshot 8. Snapshot 9 shows the instant where the liquid column has reached its maximum displacement upwards, and all the gas bubbles have nearly merged in a single bubble with a liquid film wetting the inner pipe wall. This regime can be defined by [15] and [16] as annular flow.

From now on, the liquid column starts to move back towards the bottom end and the front can be seen again coming from the top of snapshot 10. As the front moves downwards, the multiphase bubble is compressed with a minor presence of foam pockets as observed in snapshot 11. Finally, in snapshot 12 the liquid front reaches again the bottom end and a new pressure rise takes place, which condenses once more the liquid vapor and compresses the NCG. This situation is analogous to the one represented in snapshot 5. The column separation and the later impact at the bottom end defines the time delay between peaks.

The same snapshot representation is also used for the other test liquids used in this study. The flow visualization with deaerated ethanol is presented in figure 5 and with deaerated acetaldehyde in figure 6, where one can distinguish the same flow sequence described previously with water. The main difference observed comes from the nature of the multiphase bubble during column separation, mainly in snapshots 8 and 9. Now, the initial foamy mixture does not become the unique bubble found with water. Instead, the whole volume left during column separation is filled with a bubbly flow. The same behavior is observed in the flow visualization made with acetaldehyde in figure 6. Once more, snapshots 8 and 9 show the volume filled with a bubbly flow. Acetaldehyde and ethanol share nearly the same surface tension ($\sigma = 21.2\,mN/m$ and $\sigma = 22.27\,mN/m$ for acetaldehyde and ethanol, respectively, and $\sigma = 72.85\,mN/m$ for water) that may explain the similar behavior observed during column separation. Indeed, the Hinze's scale proposed by [17] shows the lower the surface tension of the liquid, the easier the transition to dispersed bubble regime. This would explain the behavior observed in the multiphase bubble with deaerated ethanol and deaerated acetaldehyde, which is not found with water.

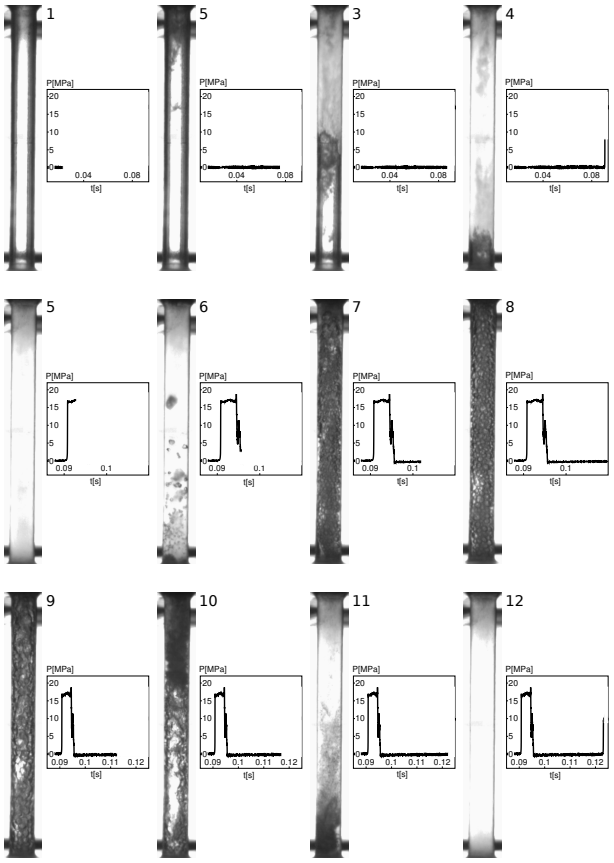

Figure 6. Liquid front visualization obtained with deaerated acetaldehyde in the straight configuration. Test conditions: $P_T = 2\,MPa$ *and* $P_p = 1\,kPa$

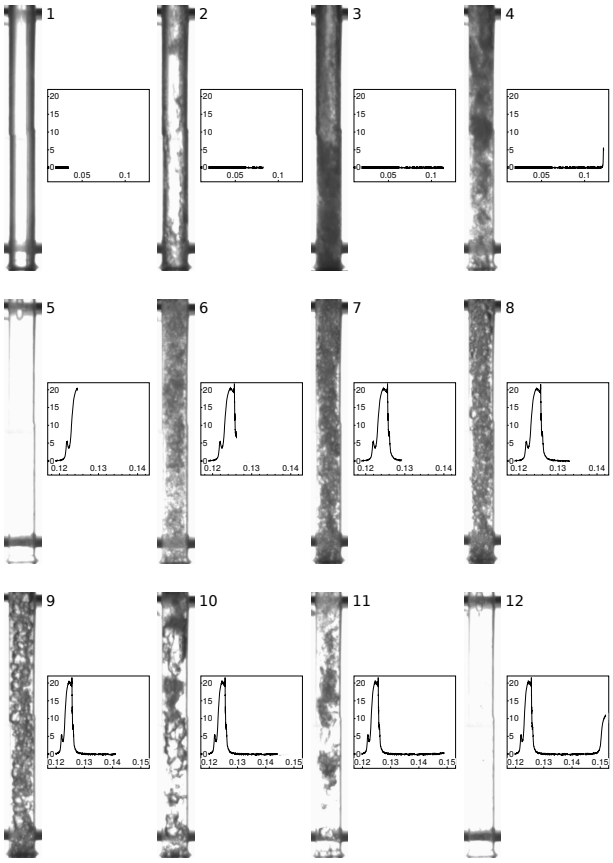

Figure 7. Liquid front visualization obtained with saturated water in the straight configuration. Test conditions: $P_T = 2\,MPa$ *and* $P_p = 1\,kPa$

4.2. Results with saturated liquids

Liquids under saturation conditions are drastically affected by the dissolved gas phase during fluid hammer occurrence, mainly when the liquid experiences a high desorption rate. The authors concluded in [14] that in liquids with a low gas desorption rate, as water, the dissolved gas phase hardly affects the fluid hammer phenomenon. For this reason, water visualizations shown in figure 7 offers nearly the same flow sequence as represented in figure 4.

On the other hand, saturated ethanol and acetaldehyde experience an intense gas desorption rate during fluid hammer occurrence, damping the pressure level and shortening the attenuation process. As a consequence of this behavior, the flow patterns observed in figures 8 and 9 change completely, mainly because column separation does not take place. The massive arrival of evolved NCG not only decreases the initial pressure rise, but also adds compressibility to the fluid, allowing the movement of the liquid column towards the tank by expanding the volume of gas bubble mixed within the liquid. Furthermore, the foamy mixture that now precedes the acetaldehyde front arrival, which was not observed when $P_p = 1\,kPa$, indicates that gas desorption already starts during FOV opening.

Figures 8 and 9 illustrate this description, where the NCG volumes compress and expand according to the traveling pressure waves, but the liquid column is never detached from the bottom end.

5. CONCLUSIONS

This work describes an experimental approach to study the priming process taking place in satellites. The experimental facility proposed in this study reproduces the fluid hammer produced during priming, with inert fluids replacing the highly toxic MMH and NTO. The facility allows flow visualizations recorded during fluid hammer occurrence by means of high speed imaging. The aim is to analyze the multiphase nature of the flow during fluid hammer occurrence.

The presentation of the results with a sequence of snapshots allows distinguishing the foamy mixture

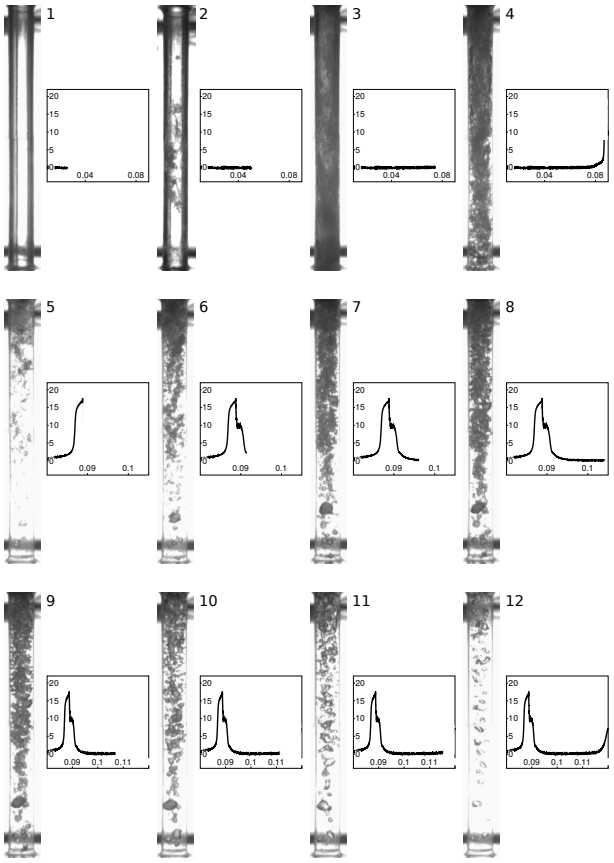

Figure 8. Liquid front visualization obtained with saturated ethanol in the straight configuration. Test conditions: $P_T = 2\,MPa$ *and* $P_p = 1\,kPa$

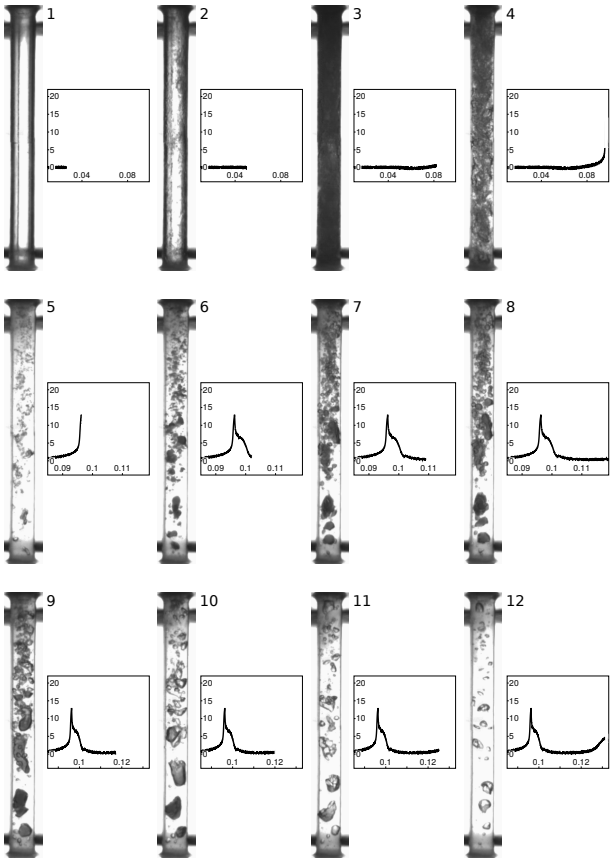

Figure 9. Liquid front visualization obtained with saturated acetaldehyde in the straight configuration. Test conditions: $P_T = 2\,MPa$ *and* $P_p = 1\,kPa$

preceding the liquid front and the NCG compression when the front impacts at the bottom end, the subsequent column separation with the creation of a multiphase bubble, ending with a new impact of the separated liquid column against the bottom end. The nature of the multiphase bubble is different for the three liquids : water leaves an annular flow behind the column, while ethanol and acetaldehyde induce a bubbly flow. The lower surface tension of these two liquids would explain this behavior. Finally, liquid column separation does not take place when ethanol and acetaldehyde are tested under saturated conditions, since gas desorption is very effective in these liquids and the growing amount of evolved NCG in the line drastically increases the fluid compressibility.

ACKNOWLEDGMENTS

This study was supported by the European Space Agency through the GSTP activity AO/1-6210/09/NL/CP.

REFERENCES

1. K L Yaggy. Analysis of propellant flow into evacuated and pressurized lines. In *20th AIAA/SAE/ASME Joint Propulsion Conference and Exhibit*, 1984.

2. R P Prickett, E Mayer, and J Hermal. Water hammer in a spacecraft propellant feed system. *Journal of Propulsion and Power*, 8(3):592–597, 1992.

3. J Molinsky. Water hammer test of the seastar hydrazine propulsion system. In *33rd AIAA/ASME/SAE/ASEE Joint Propulsion Conference & Exhibit*, 1997.

4. T Martin, L Rockwell, and C Parish. Test and modeling of the mars '98 descent propulsion system waterhammer. In *34rd AIAA/ASME/SAE/ASEE Joint Propulsion Conference & Exhibit*, 1998.

5. Chang Yeol Joh and Kum Dang Park. Pressure surge analysis and reduction in the kompsat propellant feed system. In *Proceedings KORUS 2000. The 4th Korea-Russia International Symposium on Science and Technology*, 2000.

6. Michael J. Morgan. Pressure transient characterization test for star-2 propulsion system fuel manifold. In *40th AIAA/ASME/SAE/ASEE Joint Propulsion Conference and Exhibit*, 2004.

7. T Y Lin and D Baker. Analysis and testing of propellant feed system priming process. *Journal of Propulsion and Power*, 11(3):505–512, 1995.

8. J Navickas, W C Rivard, A R Porter, D L Baker, and K A Rathgeber. Structural pressures developed during fill of evacuated systems. In *AIAA, Fluid Dynamics Conference*, 1996.

9. Laurent Ounougha and Fabrice Colozzi. Correlation between simulations and experiments on water hammer effect in a propulsion system. In *Proceedings of Second Eurpean Spacecraft Propulsion Conference*, 1997.

10. Charles Leca and Philippe Boh. Mon and mmh pressure surges for a simplified propellant feed system. In *proceedings of* 3^{rd} *international conference on spacecraft propulsion, Cannes, France*, December 2000.

11. Henry C Hearn. Development and application of a priming surge analysis methodology. In *41st AIAA/ASME/SAE/ASEE Joint Propulsion Conference & Exhibit*, 2005.

12. I. Gibek and Y. Maisonneuve. Waterhammer tests with real propellants. In *proceedings of 41st AIAA/ASME/SAE/ASEE Joint Propulsion Conference & Exhibit, Tucson (AZ), USA, 10-13 July*, number 2005–4081, 10-13 July 2005.

13. R. Lecourt and J. Steelant. Experimental investigation of water hammer in simplified feed lines of satellite propulsion systems. *Journal of Propulsion and Power*, 23(6):1214–1224, 2007.

14. Marcos Lema, Fernando López Peña, Patrick Rambaud, Jean-Marie Buchlin, and Johan Steelant. Fluid hammer with gas desorption in a liquidfilling tube: experiments with three different liquids. *Experiments in Fluids*, 56(9):180 – 192, September 2015.

15. J Weisman. *Two-phase flow patterns*, chapter 15 in Handbook of Fluids in Motion, pages 409–425. Ann Arbor Science, 1983.

16. Christopher E Brennen. *Fundamentals of multiphase flow*. Cambridge University Press, 2005.

17. J O Hinze. Fundamentals of the hydrodynamic mechanism of splitting in dispersion processes. *A.I.Ch.E. Journal*, 1(1):289–295, 1955.